ACS SyntheticBiology

Research Article

pubs.acs.org/synthbio

A Prototype for Modular Cell Engineering

Brandon Wilbanks, Donovan S. Layton, Sergio Garcia, and Cong T. Trinh*

Department of Chemical and Biomolecular Engineering, University of Tennessee, Knoxville, Tennessee 37996, United States

Supporting Information

ABSTRACT: When aiming to produce a target chemical at high yield, titer, and productivity, various combinations of genetic parts available to build the target pathway can generate a large number of strains for characterization. This engineering approach will become increasingly laborious and expensive when seeking to develop desirable strains for optimal production of a large space of biochemicals due to extensive screening. Our recent theoretical development of modular cell (MODCELL) design principles can offer a promising solution for rapid generation of optimal strains by coupling a modular cell with exchangeable production modules in a plug-and-play fashion. In this study, we experimentally validated some design properties of MODCELL by demonstrating the following: (i) a modular (chassis) cell is required to couple with a production module, a heterologous ethanol pathway, as a testbed, (ii) degree of coupling between the modular cell and production modules can be modulated to enhance growth and product synthesis, (iii) a modular cell can be used as a host to select an optimal pyruvate decarboxylase (PDC) of the ethanol production module and to help identify a hypothetical PDC protein, and (iv) adaptive laboratory evolution based on growth selection of the modular cell can enhance growth and product synthesis rates. We envision that the MODCELL design provides a powerful prototype for modular cell engineering to rapidly create optimal strains for synthesis of a large space of biochemicals.

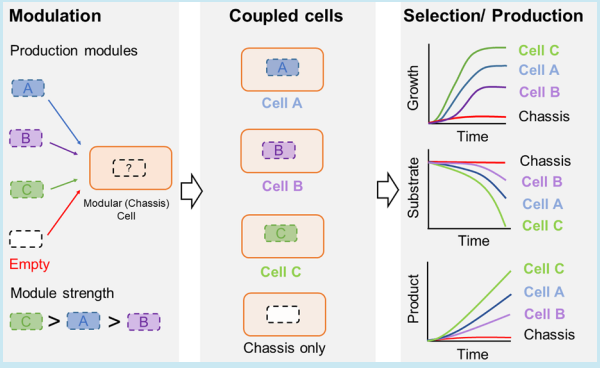

KEYWORDS: *modular cell, MODCELL, growth selection, production module, growth coupling, pyruvate decarboxylase, ethanol, adaptive laboratory evolution*

Downloaded via UNIV OF TENNESSEE KNOXVILLE on February 3, 2019 at 02:47:12 (UTC).
See https://pubs.acs.org/sharingguidelines for options on how to legitimately share published articles.

Cellular metabolisms are diverse and complex, encompassing a substantial space of chemicals.[1,2] Harnessing these cellular metabolisms for biocatalysis provides a promising path to industrialization of biology that can potentially synthesize these chemicals from renewable feedstocks and organic wastes.[3−5] To achieve this, it is necessary to rewire cellular metabolisms to achieve production efficiency in a rapid and controllable fashion.

Metabolic engineering and synthetic biology are shaping industrialization of biology. A variety of model-guided tools have been developed to enable rational strain engineering that guide desirable genetic knockouts, knock-ins, and up/down expression systems for redirecting metabolic fluxes to desirable engineered pathways, with applications ranging from production of industrially relevant bulk chemicals to specialty products and drugs.[6−15] Synergistically, synthetic biology has offered a wide range of genetic tools to engineer promoters,[16−18] ribosome binding sites,[19] terminators,[20,21] plasmid copy numbers,[22,23] regulatory and sensory elements,[24−26] and genetic circuits[27,28] for controlling metabolic fluxes. With advancement in DNA sequencing, gene synthesis, and pathway assembly, strain variants can be rapidly built and subsequently tested for efficient chemical production.[29,30−33] The current limitation, however, is to screen for a large space of strain variants through multiple design−build−test cycles of strain optimization to achieve a desirable production phenotype.[5] When expanding to produce a large space of desirable chemicals, the current strain engineering approach will become increasingly laborious and expensive.

Modular design offers the most efficient route for rapid and systematic production that has been applied in most aspects of our modern society, from constructing houses and buildings to transportation systems, industrial factories, and intricate communication networks. Remarkably, biological systems also follow modular design principles,[34−37] and exploiting these principles can potentially facilitate rapid and systematic generation of optimal strains to produce a large space of biochemicals,[1,38] a promising path toward industrialization of biology. Recent advances in metabolic engineering have significantly progressed to enable modular design of synthetic pathways for combinational biosynthesis of chemicals and fuels.[3,8,39−43] However, a prototype for modular cell engineering is still underdeveloped for generating a desirable modular (chassis) cell that is most compatible with pathway modules to achieve most desirable production phenotypes with minimal strain engineering efforts.

A theoretical framework for the modular cell (MODCELL) design has recently been developed to enable modular cell engineering.[44] On the basis of the MODCELL design

Received: July 31, 2017
Published: October 10, 2017

© 2017 American Chemical Society

DOI: 10.1021/acssynbio.7b00269
ACS Synth. Biol. 2018, 7, 187−199

principles, an optimal production strain can be rapidly assembled from a modular (chassis) cell and an exchangeable production module, requiring minimal strain optimization cycles. A modular cell is designed to be auxotrophic, containing core metabolic pathways that are necessary but insufficient to support cell growth and maintenance. To function, the modular cell must couple with an exchangeable production module containing an auxiliary pathway that can complement cell growth and enhance production of a target molecule. The stronger the coupling between a modular cell and an exchangeable production module, the faster the coupled cell grows, consumes a substrate(s), and efficiently produces a target chemical(s).[1] The production module is required to balance redox, energy, and intracellular metabolites of the modular cell for sustained cellular metabolism during growth and/or stationary phases.

In this study, we experimentally validated some design properties of MODCELL, a prototype for modular cell engineering. We showed that a modular (chassis) cell is required to couple with a production module, using a heterologous ethanol pathway, as a testbed. By varying the strengths of production modules, we illustrated the degrees of coupling between the modular cell and production modules can be modulated to enhance growth and product synthesis. We further demonstrated a modular cell can be used as a host to select an optimal pyruvate decarboxylase (PDC) of the ethanol production module and to help identify a hypothetical PDC protein. Lastly, we illustrated that adaptive laboratory evolution based on growth selection of the modular cell can enhance growth and target product synthesis rates.

RESULTS AND DISCUSSION

Characterizing Design Properties of a Modular Cell and Production Modules. To validate the MODCELL design, we first constructed the modular cell TCS095 (DE3), derived from TCS083,[45] containing 10 genetic modifications including chromosomal disruption of *pta* (encoding phosphate acetyl transferase), *poxB* (encoding pyruvate oxidase), *ldhA* (encoding lactate dehydrogenase), *adhE* (encoding alcohol dehydrogenase), *zwf* (encoding glucose-6-phosphate dehydrogenase), *ndh* (encoding NADH:quinone oxidoreductase II), *frdA* (encoding fumarate reductase), and *sfcA/maeB* (encoding malate enzyme) as well as chromosomal integration of T7 polymerase gene. The employed gene knockouts were determined on the basis of MODCELL predictions,[44] which directs design of the modular cell as a proper chassis for selection of a given pathway. MODCELL is capable of efficiently guiding a researcher with a chassis design that is otherwise not immediately intuitive. This modular cell is a prototype of MODCELL1 that is designed to strongly couple with exchange production modules for producing alcohols (ethanol, butanol, isobutanol) and esters (ethyl butyrate, isobutyl butyrate, and butyl butyrate).[44] MODCELL1 is auxotrophic under anaerobic conditions due to imbalance of redox and precursor metabolites required for cell synthesis. To validate some properties of MODCELL, we focused on design, construction, and characterization of various ethanol production modules (Figure 1).

We first built the ethanol module, pDL023, a two-operon, two-gene pathway, that is comprised of a pyruvate decarboxylase gene pdc_{ZM}, derived from *Zymomonas mobilis*, to convert pyruvate to acetaldehyde and an alcohol dehydrogenase gene $adhB_{ZM}$ to convert acetaldehyde to ethanol. We also

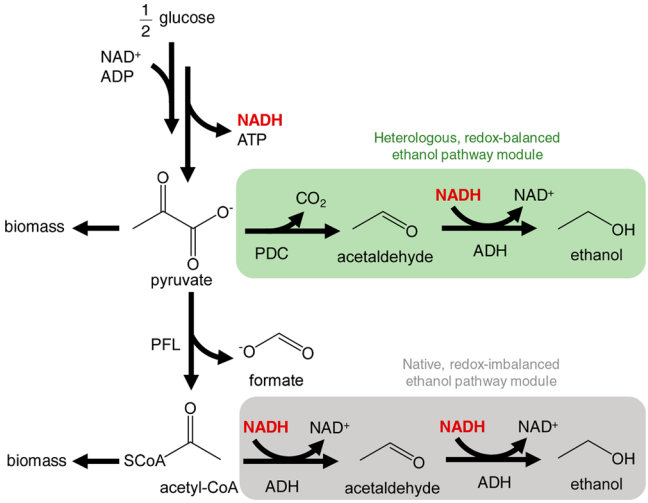

Figure 1. Homoethanol pathways for modular cell selection. The pathway highlighted in green is heterologous and redox-balanced that can couple with the modular cell, TCS095 (DE3) or TCS083 (DE3), to enable cell growth under anaerobic conditions. The pathway highlighted in gray is native but redox-unbalanced, which does not enable growth under anaerobic conditions using the modular cell.

constructed the incomplete ethanol production modules only containing either pdc_{ZM} (pCT15) or $adhB_{ZM}$ (pCT022). By transforming pCT15, pCT022, and pCT023 into TCS095 (DE3), we generated the coupled cells EcDL107, EcDL108, and ECDL109, respectively (Figure 2A).

Strain characterization showed that the engineered modular cell TCS095 (DE3) indeed could not grow anaerobically while the coupled cell EcDL109 (carrying the complete ethanol production module pDL023) could grow with a specific growth rate of 0.18 ± 0.01 (1/h) and reach a maximum optical density (OD, measured at 600 nm) of 1.39 ± 0.03 (Figure 2B). Furthermore, EcDL109 consumed all glucose within 24 h and mainly produced ethanol with a yield of 0.45 ± 0.00 (g ETOH/g GLC) (>90% of the theoretical limit, 0.51 g ETOH/g GLC) and a specific rate of 0.91 ± 0.02 (g ETOH/g DCW/h) (Figure 2C). As a negative control, the uncoupled cells that contained the incomplete ethanol production modules, EcDL107 (carrying pCT15) and EcDL108 (carrying pCT022), could not support cell growth (Figure 2B). Infeasible growth of EcDL107 also implies that AdhB was mainly responsible for conversion of acetaldehyde to ethanol since the native AdhE of the modular cell TCS095 (DE3) was disrupted.

Overall, these results validated the design property that the modular cell is auxotrophic due to imbalance of redox and precursor metabolites and requires strong coupling with a production module for growth and efficient production of target chemicals. This strategy of strong coupling has been previously shown for production of butanol,[46,47] isobutanol,[48] succinate,[49] short-chain esters,[3,4,39,40] isopentenol,[50] and itaconic acid[51] from glucose and for production of ethanol from glycerol.[52] Since synthesis and regulation of redox and precursor metabolites are linked within cellular metabolism, any perturbation is expected to affect redox state and precursor requirement for cell growth and maintenance.[53] The redox imbalance resulting in auxotrophy in the modular cell can be readily explained from the simplified metabolic network shown in Figure 1. For the modular cell, the endogenous ethanol pathway is insufficient to maintain redox state because the pathway requires two NADHs per 1/2 glucose while the

DOI: 10.1021/acssynbio.7b00269
ACS Synth. Biol. 2018, 7, 187−199

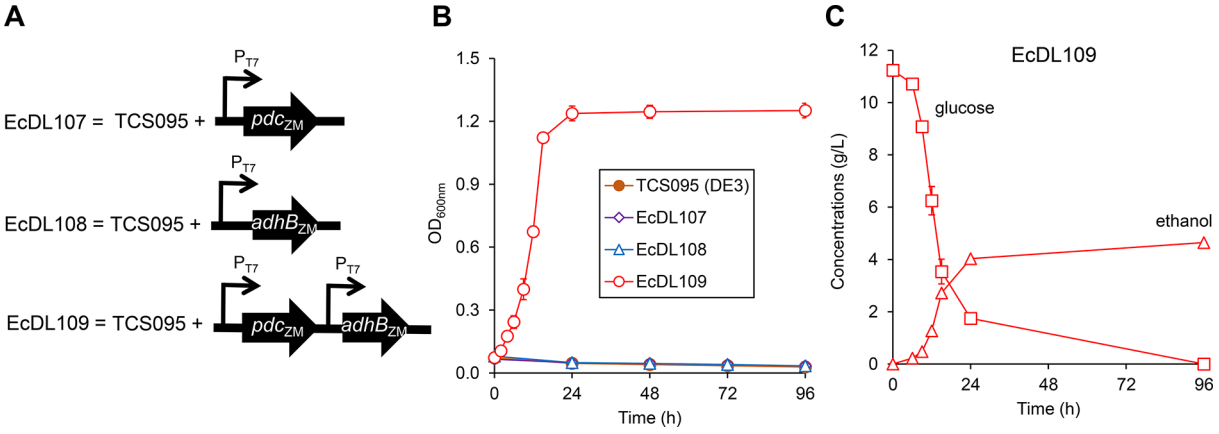

Figure 2. Strong coupling between the modular cell TCS095 (DE3) and ethanol production modules. (A) Coupled cells EcDL107, EcDL108, and EcDL109 assembled by the modular cell TCS095 (DE3) and ethanol production modules. (B) Cell growth. (C) Ethanol production and glucose consumption profiles of EcDL109. The modular cell TCS095 (DE3) and uncoupled cells, EcDL107 and EcDL108, contain incomplete ethanol modules (negative control) while EcDL109 carries a complete two-operon, two-gene ethanol module (test).

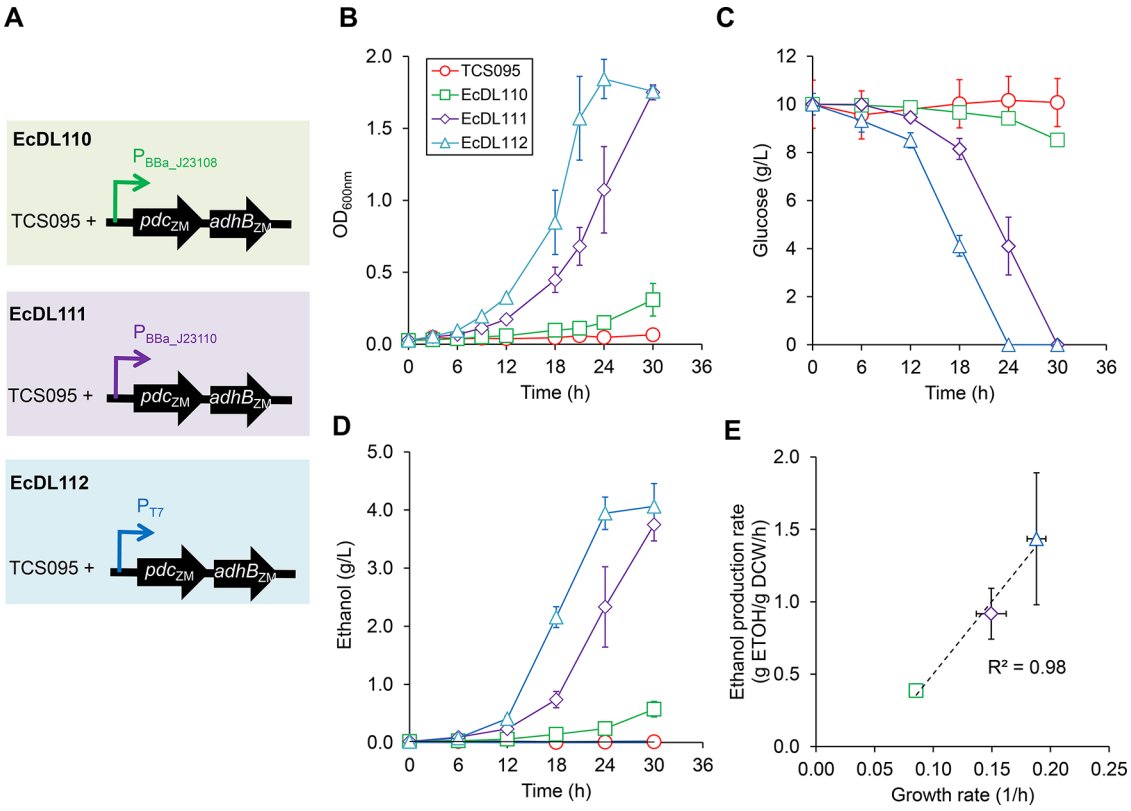

Figure 3. Modulation of degrees of coupling between the modular cell TCS095 (DE3) and ethanol production modules. (A) Coupled cells EcDL110, EcDL111, and EcDL112 assembled from the modular cell TCS095 (DE3) and the one-operon, two-gene ethanol production modules, pCT24, pAY1, and pAY3, using promoters of different strengths. (B) Cell growth. (C) Glucose consumption. (D) Ethanol production. (E) Correlation of growth and ethanol production rates.

glycolysis only produces half of the necessary cofactors. Also, strains carrying a deletion of the bifunctional aldehyde/alcohol dehydrogenase AdhE of the ethanol pathway can not grow due to underutilization of the NADH cofactor generated from glycolysis. In essence, selection of production modules by the modular cell works as antibiotics but links directly to desirable production phenotypes.

Modulating Degrees of Coupling of Modular Cell and Production Modules To Enhance Cell Growth and Product Synthesis. To further demonstrate whether degrees of coupling of the modular cell and production modules can be modulated to enhance cell growth and product formation, we constructed three one-operon, two-gene ethanol modules, with tunable strengths by varying promoters. The strongest module, pCT24, contained the strongest T7 promoter, whereas the weaker modules, pAY1 and pAY3, carried the BBa_J23100 and BBa_J23108 promoters, derived from the iGEM Andersen promoter library,[54] respectively. Among promoters in the library, BBa_J23100 was reported to have the highest strength while BBa_J23108 has 51% activity of BBa_J23100. Due to

DOI: 10.1021/acssynbio.7b00269
ACS Synth. Biol. 2018, 7, 187−199

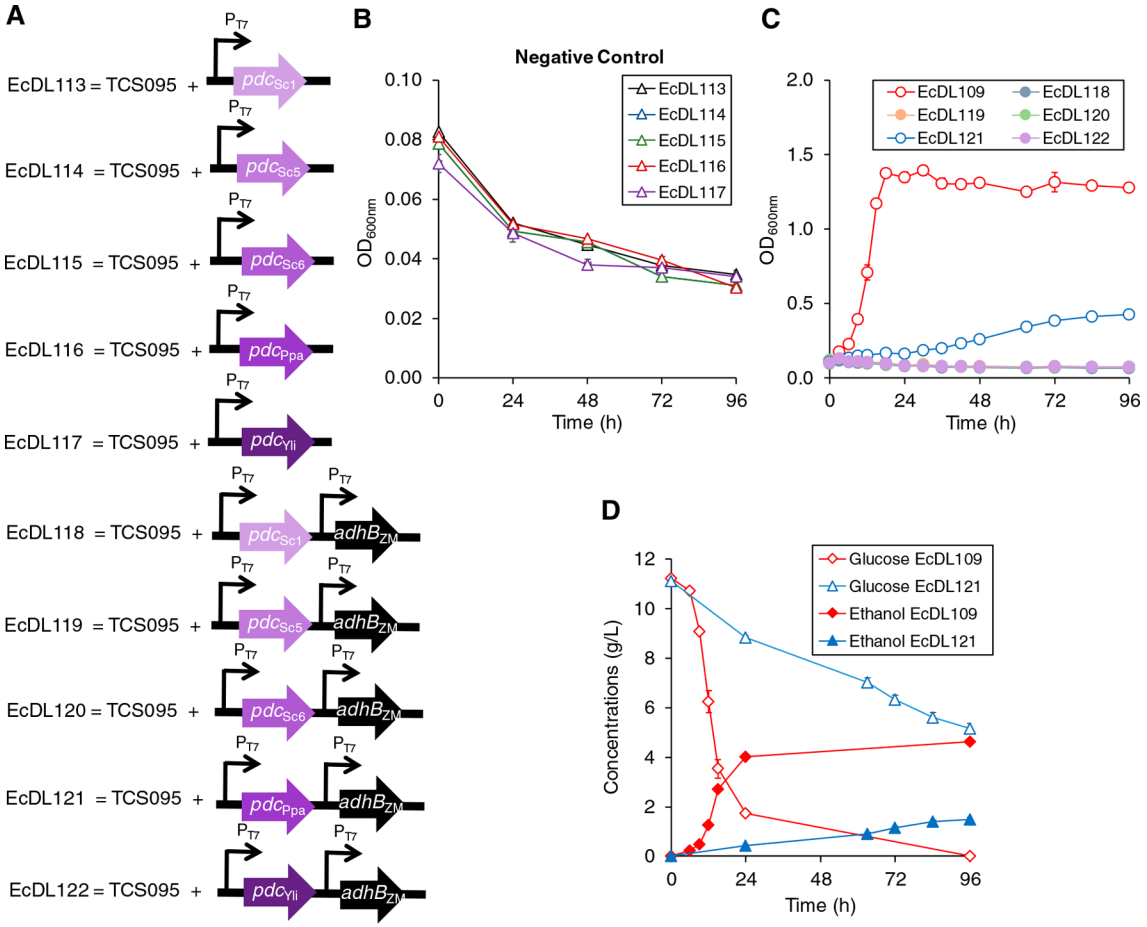

Figure 4. Selection and discovery of pyruvate decarboxylases by the modular cell TCS095 (DE3). (A) Uncoupled cells EcDL113−EcDL117 and coupled cells EcDL118−EcDL122 assembled from the modular cell TCS095 (DE3) with incomplete and complete ethanol production modules, respectively. (B) Cell growth of the modular cell TCS095 (DE3) and uncoupled cells EcDL113−EcDL117 that carry incomplete ethanol modules containing only PDCs (negative controls). (C) Cell growth of weakly coupled cells EcDL118−EcDL122 that carry complete ethanol modules containing various PDCs and the common Pdc_{ZM}. (D) Ethanol production and glucose consumption profiles of EcDL109 and EcDL121.

differences in host strains and growth conditions, we have also independently checked and confirmed the strengths of promoters used in our study: T7 ≫ BBa_J23100 ≥ BBa_J23108 (Supplementary Figure S1). We constructed three coupled cells, EcDL110, EcDL111, and EcDL112, by transforming the modules pAY3, pAY1, and pCT24 into the modular cell TCS095 (DE3), respectively (Figure 3A).

Strain characterization showed that EcDL112, carrying the module pCT24 with the strongest T7 promoter, achieved the highest growth rate of 0.19 ± 0.01 (1/h), glucose consumption rate of 3.82 ± 0.85 (g GLC/g DCW/h), and ethanol production rate of 1.44 ± 0.46 (g ETOH/g DCW/h) (Figure 3B−D). EcDL111, carrying the module pAY1 with the second strongest promoter, yielded the second highest growth rate of 0.15 ± 0.01 (1/h), glucose consumption rate of 2.48 ± 0.10 (g GLC/gDCW/h), and ethanol production rate of 0.92 ± 0.18 (g ETOH/g DCW/h) (Figure 3B−D). EcDL110, carrying the module pAY3 with the weakest promoter, obtained the lowest growth rate of 0.09 ± 0.00 (1/h), glucose consumption rate of 0.86 ± 0.28 (g GLC/g DCW/h), and ethanol production rate of 0.39 ± 0.04 (g ETOH/g DCW/h) (Figure 3B−D). Both EcDL112 and EcDL111 consumed all glucose and reached maximum ODs of 1.84 ± 0.14 and 1.75 ± 0.05, respectively, within 30 h while EcDL110 did not. In addition, we also observed a strong linear correlation (R^2 = 0.98) between growth and ethanol production rates (Figure 3E).

Taken all together, these results demonstrated that the stronger the coupling between the modular cell and ethanol production modules, the faster the coupled cells grew, consumed glucose, and produced ethanol. Coupling was able to be controlled directly by modifying metabolic fluxes through the pathway of interest. For developing prototypes for modular cell engineering, stronger production modules with balanced fluxes should be enforced to create desirable coupled cells for enhanced production of target chemicals. Production modules with imbalanced fluxes of intermediate steps can significantly affect target product yields as observed for production of isobutanol, ethyl butyrate, isopropyl butyrate, and isobutyl butyrate.[3,4,39,40,48]

Enabling Modular Cells for Enzyme Selection. *Selection of PDCs with the Modular Cell TCS095 (DE3).* Upon confirming the strong coupling between the modular cell and ethanol production module, we next tested whether the modular cell TCS095 (DE3) can be used as a selection host for a target enzyme, *i.e.*, a pyruvate decarboxylase PDC of the ethanol production module. We selected five eukaryotic PDC genes, including pdc_{Sc1}, pdc_{Sc5}, and pdc_{Sc6} of *S. cerevisiae*, pdc_{Ppa} of *P. pastoris*, and putative pdc_{Yli} of *Y. lipolytica*, that are divergently different from bacterial PDCs (*e.g.*, pdc_{ZM} of

DOI: 10.1021/acssynbio.7b00269
ACS Synth. Biol. 2018, 7, 187−199

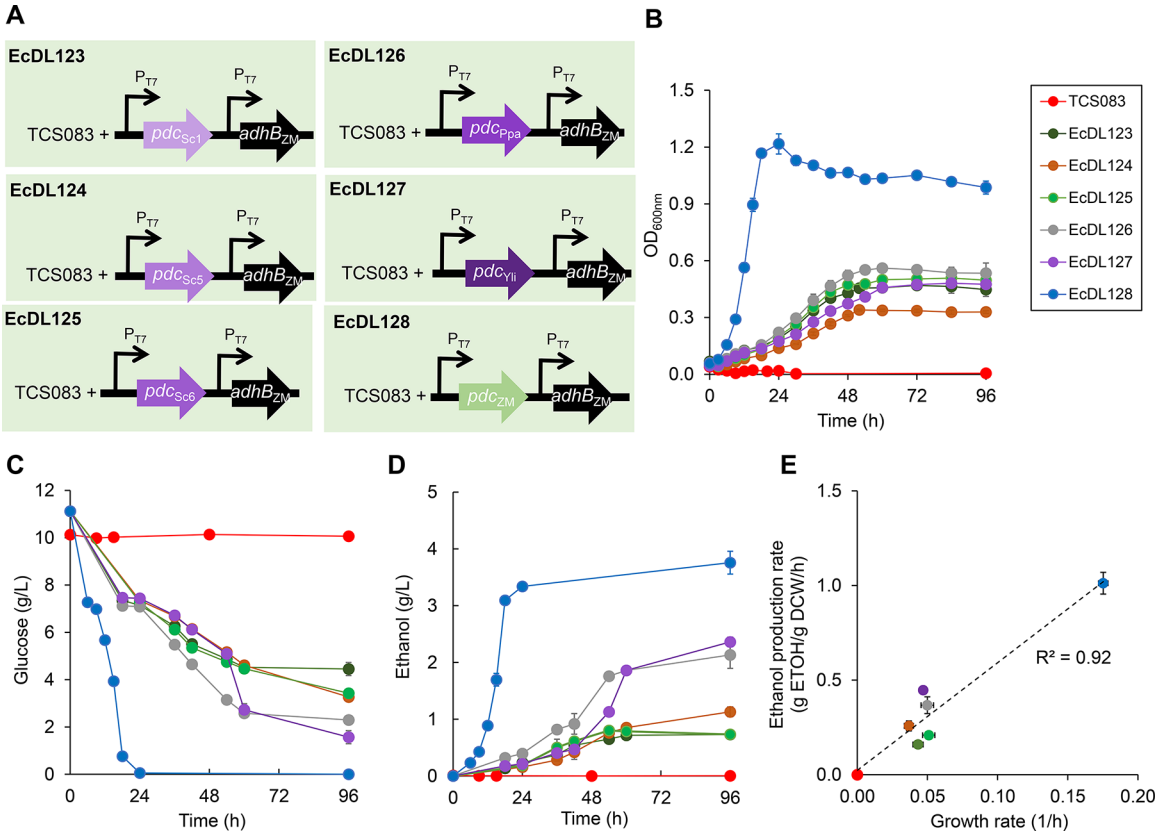

Figure 5. Selection and discovery of pyruvate decarboxylases by the modular cell TCS083 (DE3). (A) Coupled cells EcDL123−EcDL128 assembled from the modular cell TCS083 (DE3) with the two-operon, two-gene ethanol modules. (B) Cell growth. (C) Glucose consumption. (D) Ethanol production. (E) Correlation of growth and ethanol production rates.

Z. mobilis). It has been reported that the *in vitro* catalytic efficiencies of PDC_{Sc1}, PDC_{Sc5}, PDC_{Sc6} and PDC_{Ppa} are relatively similar but significantly lower than that of the bacterial PDC_{ZM} (Supplementary Figure S2).[55] The activity of putative PDC_{Yli} is widely unknown, which makes it a good candidate to test the selection capability of the modular cell. Should the putative PDC_{Yli} have the predicted function, the coupled cell carrying the PDC_{Yli}-dependent ethanol module will grow and produce ethanol; the stronger the activity of PDC_{Yli}, the faster the coupled cell will grow and produce ethanol.

We created a library of five two-operon, two-gene ethanol production modules in which we varied the PDC genes and fixed a relatively strong $AdhB_{ZM}$ gene. The complete ethanol production modules, including pDL024, pDL025, pDL026, pDL027, and pDL028, contained pdc_{Sc1}, pdc_{Sc5}, pdc_{Sc6}, pdc_{Ppa} and pdc_{Yli}, respectively, together with the common $adhB_{ZM}$ gene. By transforming these modules into the modular cell TCS095 (DE3), we constructed the coupled cells EcDL118, EcDL119, EcDL120, EcDL121, and EcDL122, respectively (Figure 4A). For negative controls, we also built the incomplete ethanol modules, including pCT15, pDL017, pDL018, pDL019, pDL020, and pDL021, that contained only pdc_{Zm}, pdc_{Sc1}, pdc_{Sc5}, pdc_{Sc6}, pdc_{Ppa} and pdc_{Yli}, respectively, without the $AdhB_{ZM}$ gene. The uncoupled cells carrying these incomplete ethanol modules are EcDL107, EcDL113, EcDL114, EcDL115, EcDL116, and EcDL117, respectively (Figure 4A).

Strain characterization showed that both the negative and positive controls were confirmed. Specifically, the positive control strain EcDL109 grew (Figure 4C) while the negative control strains, including TCS095 (DE3), EcDL107, and EcDL113−EcDL117, could not (Figure 4B). For the test experiments, only the coupled cell EcDL121 containing PDC_{Ppa} grew (Figure 4C). EcDL121 (0.02 ± 0.00 1/h) grew much slower than EcDL109 (0.18 ± 0.01 1/h) with lower glucose consumption rate (0.51 ± 0.01 g GLC/g DCW/h) and ethanol production rate (0.13 ± 0.00 g ETOH/g DCW/h) (Figure 4D) mainly because EcDL121 carried a much weaker ethanol production module than EcDL109 (*i.e.*, $PDC_{ZM} \gg PDC_{PPa}$). Further, EcDL121 only grew up to a maximum OD of 0.42 ± 0.03, ~3.3 fold less than EcDL109, and did not completely consume glucose within 96 h.

Even though some eukaryotic PDC_{Sc1}, PDC_{Sc5}, and PDC_{Sc6} were previously reported to have higher *in vitro* catalytic efficiencies than PDC_{Ppa},[55] the coupled cells, EcDL118, EcDL119, and EcDL120, containing these PDCs could not grow. These observed phenotypes could have been caused by nonoptimized translation of these eukaryotic PDC genes and/or inefficient *in vivo* enzymatic activities in the heterologous host. As a result, the selection pressure by TCS095 (DE3) might have been too strong for the weak ethanol modules containing these eukaryotic PDCs. The very weak coupling between the modular cell and the modules likely caused the imbalance of redox and precursor metabolites (*e.g.*, pyruvate, acetyl CoA) and hence inhibited growth of some coupled cells carrying weak eukaryotic PDCs.

Selection of PDCs with the Modular Cell TCS083 (DE3). To be able to detect the *in vivo* activities of PDC_{Sc1}, PDC_{Sc5}, PDC_{Sc6}, and PDC_{Yli}, it is necessary to reduce the strength of selection of TCS095 (DE3). Our strategy was to allow the

DOI: 10.1021/acssynbio.7b00269
ACS Synth. Biol. 2018, 7, 187−199

native, bifunctional acetaldehyde/ethanol dehydrogenase AdhE to relieve redox and/or acetylCoA imbalance that eukaryotic PDCs of the weak ethanol modules alone could not overcome. On the basis of the MODCELL design, TCS083 (DE3), which is the parent of the modular cell TCS095 (DE3) and still possesses the native AdhE, can function as a modular cell.[44] Though the presence of this native AdhE alone is not enough to balance redox and sustain growth (Figure 5B), the expression of eukaryotic PDCs of interest in the chassis TCS083 (DE3) is expected to recover growth by correcting the imbalance. The activity of bifunctional AdhE means that TCS083 (DE3) has a less stringent metabolic environment, hence, less metabolic relief *via* PDC is sufficient to balance redox. In contrast, with monofunctional AdhB, increased levels of PDC activity are required. By coupling TCS083 (DE3) with pDL024 (containing $pdc_{Sc1}/adhB_{Zm}$), pDL025 ($pdc_{Sc5}/adhB_{Zm}$), pDL026 ($pdc_{Sc6}/adhB_{Zm}$), pDL027 ($pdc_{Ppa}/adhB_{Zm}$), and pDL028 ($pdc_{Yli}/adhB_{Zm}$), we constructed the coupled cells EcDL123, EcDL124, EcDL125, EcDL126, and EcDL127, respectively (Figure 5A). The coupled cell EcDL128 carrying pDL023 ($pdc_{Zm}/adhB_{Zm}$) was used as a positive control while the modular cell TCS083 (DE3) was tested as a negative control.

Strain characterization shows that the coupled cell EcDL128 (positive control) could grow while the modular cell TCS083 (DE3) (negative control) alone could not (Figure 5B). As expected, EcDL128, carrying the strongest PDC_{Zm} demonstrated the strongest product coupling among all strains tested with the highest growth rate of 0.18 ± 0.00 (1/h), glucose consumption rate of 2.45 ± 0.07 (g GLC/g DCW/h), and ethanol production rate of 1.01 ± 0.06 g ETOH/g DCW/h (Figure 5B−5E). EcDL128 reached a maximum OD of 1.22 ± 0.05 and completely consumed glucose with an ethanol yield of ∼90% theoretical maximum value (Figure 5). It is interesting to observe that the performance of EcDL128 (derived from TCS083 (DE3)) is very similar to that of EcDL109 (derived from TCS095 (DE3)), which indicates that AdhB alone is sufficiently strong to support the turnover of all necessary acetaldehyde in the ethanol production modules designed.

Using TCS083 (DE3) as the modular cell, all weakly coupled cells were able to grow. EcDL125, EcDL126, and EcDL127 grew at a similar rate of ∼0.05 (1/h), and slightly faster than EcDL123 (0.04 ± 0.00 1/h) and EcDL124 (0.04 ± 0.00 1/h). As compared to EcDL128, these strains grew ∼3.4−4.8 fold slower, did not completely consume glucose within 96 h, and reached lower maximum ODs of ∼0.34−0.56, mainly due to weak ethanol production modules (Figure 5B−5D). Similarly, all TCS083-derived, weakly coupled cells yielded ethanol production rates of ∼2.3−6.4 fold lower than the control EcDL128 (1.01 ± 0.06 g ETOH/g DCW/h) (Figure 5E). We also observed a strong correlation (R^2 = 0.92) between specific growth rates and ethanol production rates of coupled cells carrying ethanol production modules derived from different PDCs. Notably, *Y. lipolytica* PDC was demonstrated for the first time to have *in vivo* activity as observed by ethanol production in EcDL127.

Native AdhE in the Modular Cell TCS083 (DE3) Is Sufficient to Facilitate PDC Selection. We further examined whether the native AdhE alone in TCS083 (DE3) was sufficient for the modular cell to select eukaryotic PDCs that are much weaker than PDC_{ZM}. We constructed EcDL129, EcDL130, EcDL131, EcDL132, EcDL133, and EcDL134 by introducing pCT15 (containing pdc_{ZM}), pDL017 (pdc_{Sc1}), pDL018 (pdc_{Sc5}), pDL019 (pdc_{Sc6}), pDL020 (pdc_{Ppa}), and pDL021 (pdc_{Yli}) in TCS083 (DE3), respectively (Supplementary Figure S3A). While the modular cell TCS083 (DE3) (negative control) could not grow, all coupled cells could even without using $AdhB_{ZM}$ (Supplementary Figure S3B). This result suggests that the endogenous AdhE was indeed sufficient and required for the ethanol production module to couple with the module cell TCS083.

EcDL129, carrying the strongest PDC_{ZM}, grew much faster than the weakly coupled cells carrying the eukaryotic PDCs by ∼2.1−2.7 folds. Interestingly, all weakly coupled cells EcDL130−EcDL134 exhibited very similar growth, glucose consumption, and ethanol production rates like EcDL123−EcDL127 even though they only used native AdhE without $AdhB_{ZM}$ (Supplementary Figure S3C−E). In contrast, EcDL129 underperformed EcDL128 when not using $AdhB_{ZM}$. These results suggested that AdhE helped EcDL129−EcDL134 balance redox to support cell growth. The AdhE flux (acetaldehyde + NADH + H^+ → ethanol + NAD^+), however, became limiting in EcDL129 but not in EcDL130−134 because PDC_{ZM} of EcDL129 is much stronger than eukaryotic PDCs of EcDL130−EcDL134. Further, the results implied that eukaryotic PDCs were limiting and the bifunctional acetaldehyde/alcohol dehydrogenase AdhE was critical for selection of weak ethanol production modules.

Taken all together, we validated the MODCELL design property that a modular cell can be exploited for enzyme selection and discovery. Like modification of promoter strengths, varying PDCs of the ethanol module provides an alternative method to adjust degrees of coupling between the modular cell and production modules. These couplings can be clearly evidenced by a strong linear correlation (R^2 = 0.90) between cell growth and ethanol production rates (Supplementary Figure S4A). Manipulating these degrees of coupling also generated some remarkable trends that can help establish a prototype for modular cell engineering.

The coupled cells exhibited optimal growth and ethanol production for a coupling either between a strong modular cell (TCS095 (DE3)) and a strong ethanol module (pDL023 and pCT24) or between a less strong modular cell (TCS083 (DE3)) and a strong ethanol module. In contrast, for a coupling between a strong modular cell and a weak ethanol module (pDL024-pDL028), the coupled cells showed significantly slow to no growth and reduced ethanol production phenotypes. Growth and ethanol production were slightly improved for a coupling between a less strong modular cell and a weak ethanol module (EcDL129−EcDL134). These results underline the importance of balancing push-and-pull carbon and electron fluxes. It is also critical to utilize strong production modules for modular cell engineering to pull carbon and electron fluxes from the core pathways of the modular cell to production modules.

Adaptive Laboratory Evolution of the Coupled Modular Cells. *Evolution of Weakly Coupled Cells Resulted in Enhanced Growth and Ethanol Production Rates.* Due to the strong coupling between the modular cell and production modules, we examined whether the adaptive laboratory evolution[52,56,57] based on the growth selection of the modular cell could enhance growth and ethanol production rates of the weakly coupled cells EcDL130−EcDL134. We performed the evolution by continuously transferring cultures of EcDL130−EcDL134 during logarithmic cell growth though serial dilution in two biological replicates for ∼150 generations (∼45

DOI: 10.1021/acssynbio.7b00269
ACS Synth. Biol. 2018, 7, 187−199

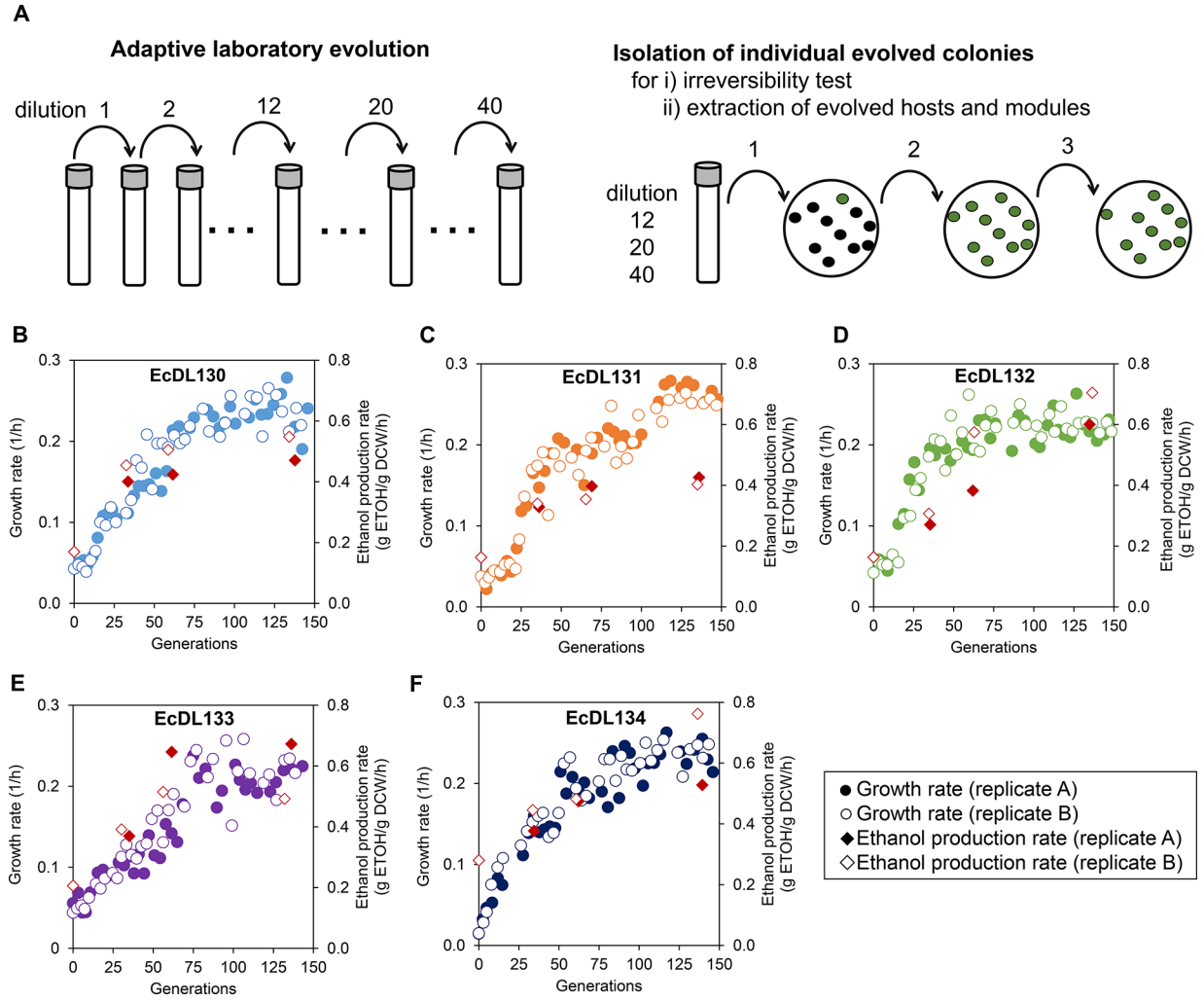

Figure 6. Adaptive laboratory evolution enhanced growth and ethanol production rates of weakly coupled cells. (A) Metabolic pathway evolution carried out by the serial culture dilution. Individual evolved cells can be isolated by serial plate spreading. Characterization of growth and ethanol production rates during the adaptive laboratory evolution of weakly coupled cells including (B) EcDL130, (C) EcDL131, (D) EcDL132, (E) EcDL133, and (F) EcDL134 for a period of 150 generations. In panels B–F, the ethanol production rates were evaluated from individual isolates from dilutions 12, 20, and 40.

transfers) (Figure 6A). For dilutions 12 (~35 generations), 20 (~60 generations), and 40 (135 generations), we also conducted the irreversibility test by isolating individual colonies of coupled cells and characterizing their performances for cell growth and ethanol production.

The results showed that the evolved EcDL130e–EcDL134e (indicated by the addition of "e" to each strain name) significantly improved growth and ethanol production rates during the adaptive laboratory evolution (Figure 6B–D). It should be noted that the letter "e" following EcDL130–EcDL134 signifies that these strains EcDL130e–EcDL134e underwent an adaptive laboratory evolution; and when a number appears after "e", it represents the number of dilution. For instance, EcDL130e40 is an evolved strain isolated at the dilution 40. For comparison and discussion hereafter, we used the performance of EcDL129 (μ = 0.10 ± 0.01 1/h and r_p = 0.48 ± 0.04 g ETOH/g DCW/h) as a benchmark because it accomplished the highest growth and ethanol production rates of all six PDCs tested before the evolution.

Initially, the weakly coupled cells EcDL130–EcDL134 grew slowly in a range of 0.04–0.05 1/h. After dilution 12, all cells significantly improved growth by ~2–4 folds, and either reached or surpassed the growth of EcDL129. Specifically, EcDL132e12 grew fastest with a growth rate of ~1.9 folds higher than the benchmark strain EcDL129. After dilution 20, all cells almost doubled the growth rate of EcDL129 where specific growth rates of EcDL130e20, EcDL131e20, EcDL132e20, EcDL133e20, and EcDL134e20 were 2.0, 1.9, 1.9, 1.6, and 2.2 folds higher than that of EcDL129, respectively. After dilution 20, coupled cells EcDL130e40–EcDL134e40 slightly improved growth where growth rates mostly reached plateau at dilution 40, ~2.0–2.6 folds higher than EcDL129. Single colony isolates at dilutions 12, 20, and 40 were also characterized for irreversibility test, and all matched the observed, enhanced growth phenotypes of evolved cultures (Supplementary Figure S5). Throughout dilution, evolved cells enhanced not only growth but also glucose consumption and ethanol production rates (Supplementary Figure S6). At dilution 40, coupled cells EcDL130e40, EcDL131e40, EcDL132e40, EcDL133e40, and EcDL134e40 reached the ethanol production rates ~3.0, 2.5, 4.0, 2.8, and 2.3 folds higher than their parents, respectively. All coupled cells either matched or slightly surpassed the ethanol production rate of EcDL129. Interestingly, we observed that there was a weak correlation

DOI: 10.1021/acssynbio.7b00269
ACS Synth. Biol. 2018, 7, 187–199

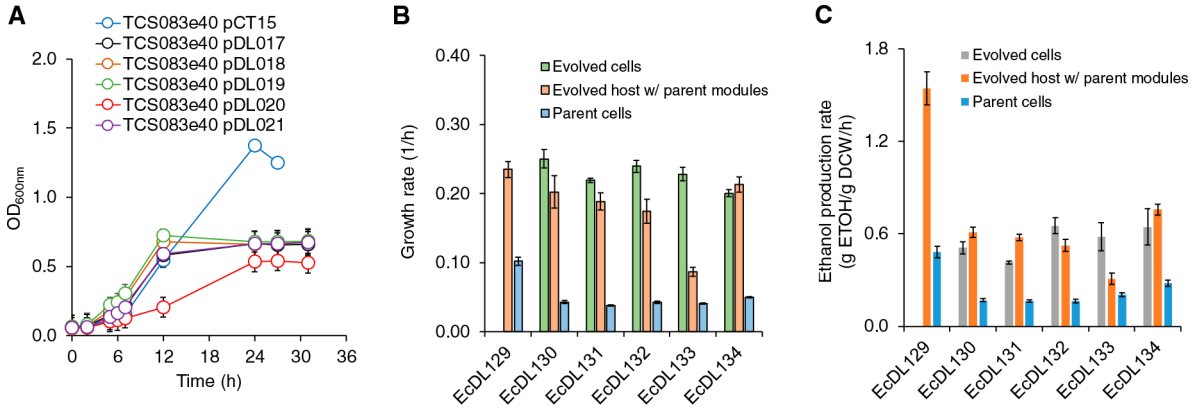

Figure 7. Adapted modular cells contributed to enhanced phenotypes of evolved cells. (A) Growth kinetics of the coupled cells assembled from the adapted modular cell carrying the parent ethanol modules including pCT15, pDL017, pDL018, pDL019, pDL020, and pDL021. The evolved modular cell TCS083e40 was isolated from EcDL133e40 at dilution 40 after rejecting pDL020. Comparison of (B) growth rate and (C) ethanol production rate among the parent coupled cells, evolved cells, and adapted modular cell carrying the parent ethanol production modules.

between growth and ethanol production rates for EcDL130–134 and their evolved derivatives at dilutions 12, 20, and 40 (Supplementary Figure S4B).

Host Adaption Contributed to Enhanced Performance of Coupled Cells. To examine whether the host or production modules contributed to enhanced phenotypes of evolved mutants, we isolated and characterized both. To characterize the evolved ethanol production modules, we selected three representative evolved cells EcDL130e40 (with PDC_{Sc1}), EcDL133e40 (with PDC_{Ppa}), and EcDL134e40 (with PDC_{Yli}), extracted their plasmids, transformed them back to the unevolved parent modular cell TCS083 (DE3), and characterized. The results showed that these coupled cells did not improve growth rates as compared to their parents (Supplementary Figure S7).

To test the host, we rejected the plasmids from the evolved cells through serial plate transfers. After multiple rounds of strain curation through plate transfers, we were able to successfully isolate TCS083e40 by rejecting the plasmid pDL020 from EcDL133e40 first and hence used it for characterization. We transformed the original modules pCT15, pDL017, pDL018, pDL019, pDL020, and pDL021 into TCS083e40 for characterization. Most coupled cells were able to regain the enhanced growth phenotypes of the evolved mutants (Figure 7A). Interestingly, TCS083e40 pCT15 doubled the growth rate of EcDL129 (TCS083 pCT15) (Figure 7B). In addition to improved growth, we also observed increase in ethanol production rates of the coupled cells derived from the evolved modular cell TCS083e40 and the original ethanol production modules (Figure 7C).

Taken all together, these results demonstrated that the modular cell can be used a selection host for adaptive laboratory evolution to enhance growth and production synthesis rates of coupled cells. The evolved EcDL130e–EcDL134e might have acquired beneficial mutations on core metabolisms of the modular cell to achieve higher growth and ethanol production rates but probably not on the production modules. Future studies will investigate the beneficial mutations through OMICS analysis and genome resequencing. Our results concured with previous studies of plasmid-bacteria evolution that plasmids tend to resist mutations even undergoing long-term (>500 generations) adaptive laboratory evolution experiments.[58,59] On the basis of this observation, to acquire beneficial mutations on the production modules, it might be necessary to generate *in vitro* module variants (*e.g.*, protein mutagenesis[60]) and use the modular cell for selection.

Unbiased Strain Classification by Principal Component Analysis Revealed Similar Emergent Features. The data generation and analysis above were supervised to validate the MODCELL design principles. To further explore an unbiased strain classification and associated features that might have emerged, we performed principal component analysis, based on a comprehensive data set including titers, rates, and yields from characterizing performances of 37 strains. These strains were derived from the parent and evolved modular cells carrying varied ethanol production modules (Supplementary Table S2). The PCA biplot divided all the strains (*i.e.*, variables) into 3 clusters based on their features (*i.e.*, measurements) (Figure 8). The cluster 1 captured all evolved, TCS083-derived strains, carrying eukaryotic PDCs, except two. This cluster was driven by the higher growth rate, glucose uptake rate, and formate titer. Additionally, evolved strains achieved higher pyruvate titers than unevolved ones (Supplementary Table S2). EcDL133* fell outside of the main evolved strain cluster due to its lower growth rate while EcDL129*, harboring PDC_{ZM},

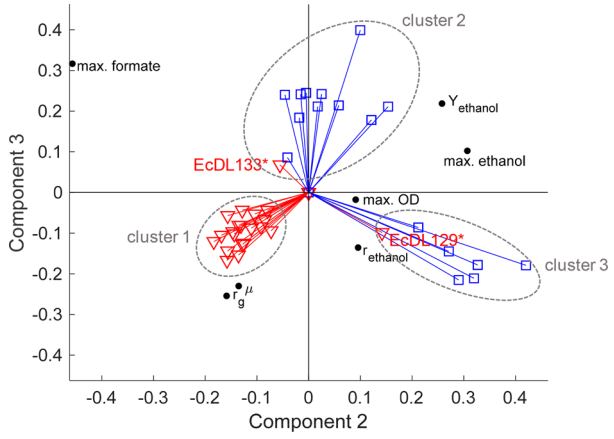

Figure 8. Classification of strain performances. PCA was performed using data presented in Supplementary Table S2, where variables correspond to strains and observations to measurements (*e.g.*, titers, rates, and yields). The vectors of evolved strains correspond to red triangles while the vectors of unevolved strains are represented by blue squares.

DOI: 10.1021/acssynbio.7b00269
ACS Synth. Biol. 2018, 7, 187–199

Table 1. List of Strains and Plasmids Used in This Study

plasmids/strains	genotypes	sources
Plasmids		
pETite*	kan^R	[39]
pCT15	pETite* P_{T7}::RBS::pdc_{Zm}::T_{T7}; kan^+	this study
pDL017	pETite* P_{T7}::RBS::$pdc1_{Sc}$::T_{T7}; kan^+	this study
pDL018	pETite* P_{T7}::RBS::$pdc5_{Sc}$::T_{T7}; kan^+	this study
pDL019	pETite* P_{T7}::RBS::$pdc6_{Sc}$::T_{T7}; kan^+	this study
pDL020	pETite* P_{T7}::RBS::pdc_{Ppa}::T_{T7}; kan^+	this study
pDL021	pETite* P_{T7}::RBS::pdc_{Yli}::T_{T7}; kan^+	this study
pDL022	pETite* P_{T7}::RBS::$adhB_{Zm}$::T_{T7}; kan^+	this study
pDL023	pETite* P_{T7}::RBS::pdc_{Zm}::T_{T7}::P_{T7}::RBS::$adhB_{Zm}$:: T_{T7}; kan^+	this study
pDL024	pETite* P_{T7}::RBS::pdc_{Sc1}::T_{T7}::P_{T7}::RBS::$adhB_{Zm}$:: T_{T7}; kan^+	this study
pDL025	pETite* P_{T7}::RBS::pdc_{Sc5}::T_{T7}::P_{T7}::RBS::$adhB_{Zm}$:: T_{T7}; kan^+	this study
pDL026	pETite* P_{T7}::RBS::pdc_{Sc6}::T_{T7}::P_{T7}::RBS::$adhB_{Zm}$:: T_{T7}; kan^+	this study
pDL027	pETite* P_{T7}::RBS::pdc_{Ppa}::T_{T7}::P_{T7}::RBS::$adhB_{Zm}$:: T_{T7}; kan^+	this study
pDL028	pETite* P_{T7}::RBS::pdc_{Yli}::T_{T7}::P_{T7}::RBS::$adhB_{Zm}$:: T_{T7}; kan^+	this study
pCT24	pETite* P_{T7}::RBS::*pdc*::RBS::*adhB*::T_{T7}; kan^+	[39]
pAY1	pETite* P_{BBa_J23100}::RBS::*pdc*:: RBS::*adhB*::T_{T7}; kan^+	this study
pAY3	pETite* P_{BBa_J23108}::RBS::*pdc*:: RBS::*adhB*::T_{T7}; kan^+	this study
Strains		
S. cerevisiae	MAT a, *ura3d0, his3-d200, leu2-d0, met15-d0*	ATCC 201388
P. pastoris	Wildtype	ATCC 28485
Y. lipolytica	MATA ura3−302 leu2−270 xpr2−322 axp2-ΔNU49 XPR2::SUC2	ATCC MYA-2613
TOP10	F-*mcrA* Δ(*mrr-hsd*RMS-*mcr*BC)Φ80*lacZ* ΔM15 Δ*lac*X74 *rec*A1 *ara*D139 Δ(*ara leu*) 7697 *gal*U *gal*K *rps*L (StrR) *end*A1 *nup*G	Invitrogen
TCS083	MG1655,ΔldhA::ΔfrdA::ΔsfcA::ΔmaeB::Δzwf::Δndh::Δpta::ΔpoxB	[45]
TCS083 (DE3)	MG1655,ΔldhA::ΔfrdA::ΔsfcA::ΔmaeB::Δzwf::Δndh::Δpta::ΔpoxB (λDE3)	this study
TCS095 (DE3)	MG1655,ΔldhA::ΔfrdA::ΔsfcA::ΔmaeB::Δzwf::Δndh::Δpta::ΔpoxB::ΔadhE (λDE3)	this study
EcDL107	TCS095 (DE3) pCT15 (pdc_{Zm}); kan^+	this study
EcDL108	TCS095 (DE3) pDL022 ($adhB_{Zm}$); kan^+	this study
EcDL109	TCS095 (DE3) pDL023 (pdc_{Zm} $adhB_{Zm}$); kan^+	this study
EcDL110	TCS095 (DE3) pAY3; kan^+	this study
EcDL111	TCS095 (DE3) pAY1; kan^+	this study
EcDL112	TCS095 (DE3) pCT24; kan^+	this study
EcDL113	TCS095 (DE3) pDL017 (pdc_{Sc1}); kan^+	this study
EcDL114	TCS095 (DE3) pDL018 (pdc_{Sc5}); kan^+	this study
EcDL115	TCS095 (DE3) pDL019 (pdc_{Sc6}); kan^+	this study
EcDL116	TCS095 (DE3) pDL020 (pdc_{Ppa}); kan^+	this study
EcDL117	TCS095 (DE3) pDL021 (pdc_{Yli}); kan^+	this study
EcDL118	TCS095 (DE3) pDL023 (pdc_{Sc1} $adhB_{Zm}$); kan^+	this study
EcDL119	TCS095 (DE3) pDL024 (pdc_{Sc5} $adhB_{Zm}$); kan^+	this study
EcDL120	TCS095 (DE3) pDL025 (pdc_{Sc6} $adhB_{Zm}$); kan^+	this study
EcDL121	TCS095 (DE3) pDL026 (pdc_{Ppa} $adhB_{Zm}$); kan^+	this study
EcDL122	TCS095 (DE3) pDL027 (pdc_{Yli} $adhB_{Zm}$); kan^+	this study
EcDL123	TCS083 (DE3) pDL023 (pdc_{Sc1} $adhB_{Zm}$); kan^+	this study
EcDL124	TCS083 (DE3) pDL024 (pdc_{Sc5} $adhB_{Zm}$); kan^+	this study
EcDL125	TCS083 (DE3) pDL025 (pdc_{Sc6} $adhB_{Zm}$); kan^+	this study
EcDL126	TCS083 (DE3) pDL026 (pdc_{Ppa} $adhB_{Zm}$); kan^+	this study
EcDL127	TCS083 (DE3) pDL027 (pdc_{Yli} $adhB_{Zm}$); kan^+	this study
EcDL128	TCS083 (DE3) pDL028 (pdc_{Zm} $adhB_{Zm}$); kan^+	this study
EcDL129	TCS083 (DE3) pCT15 (pdc_{Zm}); kan^+	this study
EcDL130	TCS083 (DE3) pDL017 (pdc_{Sc1}); kan^+	this study
EcDL131	TCS083 (DE3) pDL018 (pdc_{Sc5}); kan^+	this study
EcDL132	TCS083 (DE3) pDL019 (pdc_{Sc6}); kan^+	this study
EcDL133	TCS083 (DE3) pDL020 (pdc_{Ppa}); kan^+	this study
EcDL134	TCS083 (DE3) pDL021 (pdc_{Yli}); kan^+	this study

escaped the same cluster due to its fast growth rate and high ethanol titer, rate, and yield. The cluster 2 was represented by the TCS083- and TCS095-dereived strains carrying eukaryotic PDCs. Finally, the cluster 3 was populated by the strains harboring PDC_{ZM}, which exhibited fast growth rates and high ethanol titers, rates, and yields.

In our study, the selective pressure of the adaptive laboratory evolution using the modular cell host essentially coupled fast growth with product synthesis. Thus, the evolved strains,

DOI: 10.1021/acssynbio.7b00269
ACS Synth. Biol. 2018, 7, 187−199

carrying eukaryotic PDCs, achieved higher growth rates than the unevolved ones. To accomplish higher growth rates, these evolved strains increased their glucose uptake rates and ethanol production rates. However, the ethanol titers and yields did not improve much with observed accumulation of pyruvate and formate, which can be attributed to the weak activities of the eukaryotic ethanol production modules (Supplementary Table S2). This behavior highlights how the evolved strains were capable of adjusting their metabolisms to effectively increase growth rates and ethanol production rates but not ethanol titers and yields. Therefore, this emergent feature is important to consider for developing a prototype of modular cell engineering, *e.g.*, use of strong production modules. Further, to speed up the adaptive laboratory evolution to effectively achieve high product titers, rates and yields, it is important to build a library of production modules that contain strong variants for selection in order to avoid any potential compromise with other associated competing cellular processes.

CONCLUSION

We have developed a prototype for modular cell engineering based on the MODCELL design principles. Using a heterologous ethanol pathway as a testbed, we characterized and validated some design properties of a modular cell. We demonstrated the auxotrophy of two modular cell designs by coupling them without an ethanol module or with an incomplete ethanol module. By modulating the degrees of coupling with various promoter strengths or activities of PDCs of ethanol production modules, we demonstrated that the strong coupling is critical for enhanced growth and product formation. This strong coupling enabled the modular cell to be used as a host to select an optimal pyruvate decarboxylase (PDC) of the ethanol production module or discover the function of a hypothetical PDC protein from *Y. lipolytica*. Using the modular cell platform, adaptive laboratory evolution based on growth selection provides a simple but powerful technique to enhance growth and product rates of a targeted pathway. While this study focused on controlling the strengths of production modules by manipulating promoters, operon designs, and functional genes to validate the design properties of MODCELL, other strategies such as varying ribosome binding sites, introducing regulatory elements, and controlling gene copies *via* plasmid system or chromosome-integration can be performed. Future studies will explore these strategies and validate the plug-and-play features of the modular cell engineering to efficiently synthesize a library of molecules beyond ethanol with minimal design-build-test strain optimization cycles. We envision that MODCELL provides a powerful prototype for modular cell engineering to rapidly create optimal strains for efficient production of a large space of biochemicals and help minimize the design−build−test cycles of strain engineering.

METHODS

Strains. Table 1 lists strains used in this study. *E. coli* TOP10 was used for molecular cloning. TCS095 was constructed from TCS083[45] by deleting chromosomal gene *adhE* using P1 transduction.[61] The prophage λDE3 was used to insert a T7 polymerase gene into the specific site of TCS083 or TCS095 by using a commercial kit for strains expressing a T7 promoter (cat#69734−3, Novagen Inc.). TCS083 (λDE3), TCS095 (λDE3), and their derivatives carrying production modules were used for modular cell engineering and characterization (Table 1). All mutants and plasmids were PCR confirmed with the primers used listed in Supplementary Table S1.

Plasmid/Pathway Construction. *Construction of PDC Modules.* The pETite*, a vector backbone,[39] was used to construct PDC modules—containing PDC genes derived from *Z. mobilis*, *S. cerevisiae*, *P. pastoris*, and *Y. lipolytica* under T7 promoters—using the Gibson gene assembly method.[62] To construct the modules pDL017, pDL018, and pDL019, the genes $pdc1_{Sc}$, $pdc5_{Sc}$, and $pdc6_{Sc}$ were amplified from *S. cerevisiae* cDNA using the primers DL_0036/DL_0037, DL_0038/DL_0039, and DL_0040/DL_0041, respectively, and then inserted into the pETite* backbone isolated by using the primers DL_0001/DL_0002. Likewise, the gene pdc_{Ppa} was amplified from *P. pastoris* cDNA using the primers DL_0042/DL_0043 and inserted into the pETite* backbone, generating the module pDL020. The module pDL021 was constructed by amplifying the gene pdc_{Yli} from *Y. lipolytica* cDNA using the primers DL_0044/DL_0045 and inserted into the pETite* backbone.

The gene pdc_{ZM} was assembled into the pETite* vector to create the module pCT15 by using the BglBrick gene assembly[63] of 2 DNA pieces: (i) pdc_{ZM} amplified from the genomic DNA of *Z. mobilis* using the primers P006_f/P006_r and digested with NdeI/*Bam*HI and (ii) the vector backbone pETite* doubly digested with NdeI/*Bam*HI.

Construction of AdhB Modules. The AdhB module pDL022 was generated by amplifying the gene $adhB_{Zm}$ from pCT24 using the primers DL_0046/DL_0047 and inserted into the pETite* backbone using Gibson assembly.

Construction of the PDC and AdhB Ethanol Modules. The single-operon, PDC/AdhB ethanol module pCT24 was contructed previously.[39] Briefly, pCT24 contains the PDC and AdhB genes of the *Z. mobilis* ethanol pathway. The variant PDC/AdhB ethanol modules pAY1 and pAY3 were constructed from pCT24 by swapping the T7 promoter with two weaker constitutive promoters.[54] The module pAY1, containing the BBa_J23100 promoter, was constructed by amplifying pCT24 using the primers AY6.R/AY.7F, digesting it with *Bgl*II, and ligating it together. Likewise, the module pAY3, carrying the BBa_J23108 promoter, was constructed using the primers AY6.R/AY10.F, digesting it with *Bgl*II, and ligating it together.

In addition, we have constructed and characterized the two-operon, PDC/AdhB modules: the first operon carrying a PDC gene derived from various species and the second operon containing the $AdhB_{Zm}$ gene. The two-operon ethanol modules were constructed using the Gibson assembly method using two parts: (i) the PDC containing-plasmids, pDL017-pDL021 and pCT15, amplified using the primers DL_0013/DL_0014 and (ii) the AdhB operon amplified from pDL022 using the primers DL_0015/DL_0016 to generate pDL023-pDL028, respectively.

Medium and Cell Culturing. *Culture Media.* For molecular cloning, the lysogeny broth (LB) medium, containing 10 g/L yeast extract, 5 g/L tryptone, and 5 g/L NaCl, was used. Antibiotics at working concentrations of 50 μg/mL kanamycin (kan) was supplemented, where applicable, to maintain the selection of desired plasmids. For growth coupling experiments, the M9 (pH ∼ 7) medium was used, consisting of 100 mL/L of 10× M9 salts, 1 mL/L of 1 M $MgSO_4$, 100 μL/L of 1 M $CaCl_2$, 1 mL/L of stock thiamine HCl solution (1 g/L), 1 mL/L of stock trace metals solution,[45]

DOI: 10.1021/acssynbio.7b00269
ACS Synth. Biol. 2018, 7, 187−199

and appropriate antibiotics. Unless specified, 10 g/L glucose was used in the M9 medium. The stock 10× M9 salt solution contained 67.8 g/L Na_2HPO_4, 30 g/L KH_2PO_4, 5 g/L NaCl, and 10 g/L NH_4Cl.

Strain Characterization. Strain characterization experiments were performed by growing cells overnight at 37 °C in 15 mL culture tubes containing LB and appropriate antibiotics, then subculturing into a fresh M9 medium to adapt the cells to a defined environment. Cells were then grown until exponential phase ($OD_{600\ nm}$ ~ 1.0, 1 OD ~ 0.5 g DCW/L). Next, cells (except the modular strain TCS083 DE3) were again subcultured into a nitrogen sparged and pressured tube to create a complete anaerobic environment to an initial $OD_{600\ nm}$ ~ 0.10−0.20 at a working volume of 20 mL. The strains were allowed to adapt (at least 2 doublings) overnight to the anaerobic environment and then transferred into prewarmed 20 mL tubes dispersed of oxygen containing M9 and appropriate antibiotics for characterization with an initial $OD_{600\ nm}$ of ~0.030.

Cells were grown on a 75° angled platform in a New Brunswick Excella E25 at 37 °C and 175 rpm. Whole-cells and cell supernatants were collected and stored at −20 °C for subsequent metabolite analysis. All experiments were performed with at least three biological replicates.

Adaptive Laboratory Evolution. Strain evolution experiments were prepared and grown in an identical way to the method described above for Strain Characterization experiments. Samples for metabolite analysis were also taken in a similar manner as described in the Strain Characterization method. Upon preparation of adapted anaerobic strains, cultures were grown in duplicate from OD_{600} of ~0.050 until exponential phase was reached (OD_{600} of 0.5−1.0). A 1.5 mL sample of each replicate was collected for stock. Each replicate was then diluted to OD_{600} ~ 0.05 and grown again to an OD_{600} of 0.5−1.0, where samples were collected as before. This process was repeated until a consistent maximum growth rate was reached. Evolution was then tested for irreversibility.

When the consistent maximum growth rate was reached, cells were plated on LB plates with antibiotic as needed. A single colony was selected and streaked out on a new plate and repeated 3 times in order to ensure a single cell colony was isolated. Isolated evolved colonies were tested for irreversibility. Cells were first grown and stocked at −80 °C before conducting the experiment to allow for complete metabolic interruption and recovery. Irreversibility of the adapted host strain and adapted plasmid were carried out in the same fashion as before in the strain characterization method. Plasmids were extracted from the isolated colonies and transformed into the unevolved parent strain (TCS083 DE3) for plasmid irreversibility test. The evolved plasmid in the unevolved host was also characterized in the same method of the strain coupling studies.

Analytical Methods. *Cell Growth.* Cell optical density was directly measured by using a Thermo Scientific Genesys 30 Visible Spectrophotometer with a proper adapter to determine growth kinetics.

High Performance Liquid Chromatography (HPLC). Extracellular metabolites were quantified by first filtering cell supernatants though 0.2-μm filter units and then analyzed using the Shimadzu HPLC system equipped with RID and UV−vis detectors (Shimadzu Inc., Columbia, MD, USA) and Aminex HPX-87H cation exchange column (BioRad Inc., Hercules, CA, USA). Samples were eluded though the column set at 50 °C with a flow rate of 0.6 mL/min using the 10 mN H_2SO_4 mobile phase.[48]

Data Analysis. *Specific Growth Rate.* First-order kinetics was applied to calculate a specific growth rate from kinetic measurement of cell growth as follows:

$$\mu = \frac{1}{C_X} \cdot \frac{dC_X}{dt} \tag{1}$$

where μ (1/h) is the specific growth rate, C_X (g/L) is cell titer, and t (h) is culturing time.

Yield. A yield (Y_{Si}/Y_{Sj}) of a species S_i with respect to a species S_j ($i \# j$) was determined as follows:

$$Y_{S_i/S_j} = \frac{dC_{S_i}}{dC_{S_j}} \tag{2}$$

where C_{Si} and C_{Sj} (g/L) are concentrations of S_i and S_j, respectively.

Specific Production/Consumption Rate. A specific rate r_{Si} of a species S_i was calculated as follows:

$$r_{S_i} = \mu \cdot Y_{S_i/X} = \mu \frac{dC_{S_i}}{dC_X} \tag{3}$$

Growth Generation. The number of growth generation (n) was determined as follows:

$$n = \log_2 \frac{C_X(t_2)}{C_X(t_1)} \tag{4}$$

Principal Component Analysis. Strain performances can be classified in an unbiased manner using the principal component analysis (PCA) method. This analysis was performed on the titers, rates, and yields for all characterized strains (Supplementary Table S2). The pyruvate measurements were excluded because they were missing in several strains. The mean values were first log transformed, then PCA coefficients and scores were computed and represented in a biplot format.

■ ASSOCIATED CONTENT

Supporting Information

The Supporting Information is available free of charge on the ACS Publications website at DOI: 10.1021/acssynbio.7b00269.

Tables S1−S2; Figures S1−S7 (PDF)
Table S2 spreadsheet (XLSX)

■ AUTHOR INFORMATION

Corresponding Author

*E-mail: ctrinh@utk.edu. Tel: 865-974-8121.

ORCID

Cong T. Trinh: 0000-0002-8362-725X

Author Contributions

C.T.T. perceived and supervised the study. C.T.T., D.L., B.W. designed experiments. D.L., B.W., S.G. performed the experiments. C.T.T., D.L., B.W., S.G. analyzed the data. C.T.T. wrote the manuscript with help from all authors.

Notes

The authors declare no competing financial interest.

■ ACKNOWLEDGMENTS

We thank Akshitha Yarrabothula, Nirayan Niraula, and Katherine Krouse for helping with molecular cloning and

DOI: 10.1021/acssynbio.7b00269
ACS Synth. Biol. 2018, 7, 187−199

growth study experiments. This research was financially supported by the NSF CAREER award (NSF#1553250).

REFERENCES

(1) Trinh, C. T., and Mendoza, B. (2016) Modular cell design for rapid, efficient strain engineering toward industrialization of biology. *Curr. Opin. Chem. Eng. 14*, 18−25.
(2) National Research Council (2015) *Industrialization of Biology: A Roadmap to Accelerate the Advanced Manufacturing of Chemicals*, National Academies Press.
(3) Layton, D. S., and Trinh, C. T. (2016) Expanding the modular ester fermentative pathways for combinatorial biosynthesis of esters from volatile organic acids. *Biotechnol. Bioeng. 113*, 1764.
(4) Layton, D. S., and Trinh, C. T. (2016) Microbial synthesis of a branched-chain ester platform from organic waste carboxylates. *Metabolic Engineering Communications 3*, 245−251.
(5) Nielsen, J., and Keasling, J. D. (2016) Engineering cellular metabolism. *Cell 164*, 1185−1197.
(6) Lee, J. W., Na, D., Park, J. M., Lee, J., Choi, S., and Lee, S. Y. (2012) Systems metabolic engineering of microorganisms for natural and non-natural chemicals. *Nat. Chem. Biol. 8*, 536−546.
(7) Rodrigues, A. L., Trachtmann, N., Becker, J., Lohanatha, A. F., Blotenberg, J., Bolten, C. J., Korneli, C., de Souza Lima, A. O., Porto, L. M., Sprenger, G. A., and Wittmann, C. (2013) Systems metabolic engineering of Escherichia coli for production of the antitumor drugs violacein and deoxyviolacein. *Metab. Eng. 20*, 29−41.
(8) Ajikumar, P. K., Xiao, W.-H., Tyo, K. E. J., Wang, Y., Simeon, F., Leonard, E., Mucha, O., Phon, T. H., Pfeifer, B., and Stephanopoulos, G. (2010) Isoprenoid Pathway Optimization for Taxol Precursor Overproduction in Escherichia coli. *Science 330*, 70−74.
(9) von Kamp, A., and Klamt, S. (2017) Growth-coupled overproduction is feasible for almost all metabolites in five major production organisms. *Nat. Commun. 8*, 15956.
(10) Flowers, D., Thompson, R. A., Birdwell, D., Wang, T., and Trinh, C. T. (2013) SMET: systematic multiple enzyme targeting−a method to rationally design optimal strains for target chemical overproduction. *Biotechnol. J. 8*, 605−618.
(11) Machado, D., and Herrgård, M. (2015) Co-evolution of strain design methods based on flux balance and elementary mode analysis. *Metabol. Eng. Commun. 2*, 85.
(12) Chen, P.-W., Theisen, M. K., and Liao, J. C. (2017) Metabolic systems modeling for cell factories improvement. *Curr. Opin. Biotechnol. 46*, 114−119.
(13) Ng, C. Y., Khodayari, A., Chowdhury, A., and Maranas, C. D. (2015) Advances in de novo strain design using integrated systems and synthetic biology tools. *Curr. Opin. Chem. Biol. 28*, 105−114.
(14) Chowdhury, A., and Maranas, C. D. (2015) Designing overall stoichiometric conversions and intervening metabolic reactions. *Sci. Rep.*, DOI: 10.1038/srep16009.
(15) Wang, J., Guleria, S., Koffas, M. A. G., and Yan, Y. (2016) Microbial production of value-added nutraceuticals. *Curr. Opin. Biotechnol. 37*, 97−104.
(16) Cox, R. S., 3rd, Surette, M. G., and Elowitz, M. B. (2007) Programming gene expression with combinatorial promoters. *Mol. Syst. Biol. 3*, 145.
(17) Mutalik, V. K., Guimaraes, J. C., Cambray, G., Lam, C., Christoffersen, M. J., Mai, Q. A., Tran, A. B., Paull, M., Keasling, J. D., Arkin, A. P., and Endy, D. (2013) Precise and reliable gene expression via standard transcription and translation initiation elements. *Nat. Methods 10*, 354−360.
(18) Redden, H., and Alper, H. S. (2015) The development and characterization of synthetic minimal yeast promoters. *Nat. Commun. 6*, 7810.
(19) Salis, H. M., Mirsky, E. A., and Voigt, C. A. (2009) Automated design of synthetic ribosome binding sites to control protein expression. *Nat. Biotechnol. 27*, 946−950.
(20) Chen, Y.-J., Liu, P., Nielsen, A. A., Brophy, J. A., Clancy, K., Peterson, T., and Voigt, C. A. (2013) Characterization of 582 natural and synthetic terminators and quantification of their design constraints. *Nat. Methods 10*, 659−664.
(21) Cambray, G., Guimaraes, J. C., Mutalik, V. K., Lam, C., Mai, Q.-A., Thimmaiah, T., Carothers, J. M., Arkin, A. P., and Endy, D. (2013) Measurement and modeling of intrinsic transcription terminators. *Nucleic Acids Res. 41*, 5139−5148.
(22) Seo, J. H., and Bailey, J. E. (1985) Effects of recombinant plasmid content on growth properties and cloned gene product formation in Escherichia coli. *Biotechnol. Bioeng. 27*, 1668−1674.
(23) Karim, A. S., Curran, K. A., and Alper, H. S. (2013) Characterization of plasmid burden and copy number in Saccharomyces cerevisiae for optimization of metabolic engineering applications. *FEMS Yeast Res. 13*, 107−116.
(24) Taylor, N. D., Garruss, A. S., Moretti, R., Chan, S., Arbing, M. A., Cascio, D., Rogers, J. K., Isaacs, F. J., Kosuri, S., Baker, D., Fields, S., Church, G. M., and Raman, S. (2016) Engineering an allosteric transcription factor to respond to new ligands. *Nat. Methods 13*, 177−183.
(25) Zhang, F., Carothers, J. M., and Keasling, J. D. (2012) Design of a dynamic sensor-regulator system for production of chemicals and fuels derived from fatty acids. *Nat. Biotechnol. 30*, 354−359.
(26) Xu, P., Li, L., Zhang, F., Stephanopoulos, G., and Koffas, M. (2014) *Proc. Natl. Acad. Sci. U. S. A. 111*, 11299−11304.
(27) Nielsen, A. A., Der, B. S., Shin, J., Vaidyanathan, P., Paralanov, V., Strychalski, E. A., Ross, D., Densmore, D., and Voigt, C. A. (2016) Genetic circuit design automation. *Science 352*, aac7341.
(28) Callura, J. M., Cantor, C. R., and Collins, J. J. (2012) Genetic switchboard for synthetic biology applications. *Proc. Natl. Acad. Sci. U. S. A. 109*, 5850−5855.
(29) Jones, J. A., Vernacchio, V. R., Lachance, D. M., Lebovich, M., Fu, L., Shirke, A. N., Schultz, V. L., Cress, B., Linhardt, R. J., and Koffas, M. A. (2015) ePathOptimize: A Combinatorial Approach for Transcriptional Balancing of Metabolic Pathways. *Sci. Rep. 5*, 11301.
(30) Li, Y., Gu, Q., Lin, Z., Wang, Z., Chen, T., and Zhao, X. (2013) Multiplex iterative plasmid engineering for combinatorial optimization of metabolic pathways and diversification of protein coding sequences. *ACS Synth. Biol. 2*, 651−661.
(31) Schaerli, Y., and Isalan, M. (2013) Building synthetic gene circuits from combinatorial libraries: screening and selection strategies. *Mol. BioSyst. 9*, 1559−1567.
(32) Smanski, M. J., Bhatia, S., Zhao, D., Park, Y., L, B. A. W., Giannoukos, G., Ciulla, D., Busby, M., Calderon, J., Nicol, R., Gordon, D. B., Densmore, D., and Voigt, C. A. (2014) Functional optimization of gene clusters by combinatorial design and assembly. *Nat. Biotechnol. 32*, 1241−1249.
(33) Freestone, T. S., and Zhao, H. (2016) Combinatorial pathway engineering for optimized production of the anti-malarial FR900098. *Biotechnol. Bioeng. 113*, 384−392.
(34) Ravasz, E., Somera, A. L., Mongru, D. A., Oltvai, Z. N., and Barabási, A.-L. (2002) Hierarchical organization of modularity in metabolic networks. *Science 297*, 1551−1555.
(35) Barabasi, A.-L., and Oltvai, Z. N. (2004) Network biology: understanding the cell's functional organization. *Nat. Rev. Genet. 5*, 101−113.
(36) Han, J.-D. J., Bertin, N., Hao, T., Goldberg, D. S., Berriz, G. F., Zhang, L. V., Dupuy, D., Walhout, A. J., Cusick, M. E., and Roth, F. P. (2004) Evidence for dynamically organized modularity in the yeast protein−protein interaction network. *Nature 430*, 88−93.
(37) Newman, M. E. (2006) Modularity and community structure in networks. *Proc. Natl. Acad. Sci. U. S. A. 103*, 8577−8582.
(38) Vickers, C. E., Blank, L. M., and Krömer, J. O. (2010) Grand challenge commentary: Chassis cells for industrial biochemical production. *Nat. Chem. Biol. 6*, 875.
(39) Layton, D. S., and Trinh, C. T. (2014) Engineering modular ester fermentative pathways in *Escherichia coli*. *Metab. Eng. 26*, 77−88.
(40) Wierzbicki, M., Niraula, N., Yarrabothula, A., Layton, D. S., and Trinh, C. T. (2016) Engineering an Escherichia coli platform to synthesize designer biodiesels. *J. Biotechnol. 224*, 27−34.

DOI: 10.1021/acssynbio.7b00269
ACS Synth. Biol. 2018, 7, 187−199

(41) Tseng, H.-C., and Prather, K. L. (2012) Controlled biosynthesis of odd-chain fuels and chemicals via engineered modular metabolic pathways. *Proc. Natl. Acad. Sci. U. S. A. 109*, 17925−17930.
(42) Dellomonaco, C., Clomburg, J. M., Miller, E. N., and Gonzalez, R. (2011) Engineered reversal of the β-oxidation cycle for the synthesis of fuels and chemicals. *Nature 476*, 355−359.
(43) Cheong, S., Clomburg, J. M., and Gonzalez, R. (2016) Energy- and carbon-efficient synthesis of functionalized small molecules in bacteria using non-decarboxylative Claisen condensation reactions. *Nat. Biotechnol. 34*, 556.
(44) Trinh, C. T., Liu, Y., and Conner, D. J. (2015) Rational design of efficient modular cells. *Metab. Eng. 32*, 220−231.
(45) Trinh, C. T., Unrean, P., and Srienc, F. (2008) Minimal Escherichia coli cell for the most efficient production of ethanol from hexoses and pentoses. *Appl. Environ. Microbiol. 74*, 3634−3643.
(46) Trinh, C. T. (2012) Elucidating and reprogramming Escherichia coli metabolisms for obligate anaerobic n-butanol and isobutanol production. *Appl. Microbiol. Biotechnol. 95*, 1−12.
(47) Shen, C. R., Lan, E. I., Dekishima, Y., Baez, A., Cho, K. M., and Liao, J. C. (2011) Driving forces enable high-titer anaerobic 1-butanol synthesis in Escherichia coli. *Applied and environmental microbiology 77*, 2905−2915.
(48) Trinh, C. T., Li, J., Blanch, H. W., and Clark, D. S. (2011) Redesigning Escherichia coli metabolism for anaerobic production of isobutanol. *Applied and environmental microbiology 77*, 4894−4904.
(49) Zhang, X., Jantama, K., Moore, J. C., Jarboe, L. R., Shanmugam, K. T., and Ingram, L. O. (2009) Metabolic evolution of energy-conserving pathways for succinate production in Escherichia coli. *Proc. Natl. Acad. Sci. U. S. A. 106*, 20180−20185.
(50) Kang, A., Meadows, C. W., Canu, N., Keasling, J. D., and Lee, T. S. (2017) High-throughput enzyme screening platform for the IPP-bypass mevalonate pathway for isopentenol production. *Metab. Eng. 41*, 125−134.
(51) Harder, B.-J., Bettenbrock, K., and Klamt, S. (2016) Model-based metabolic engineering enables high yield itaconic acid production by Escherichia coli. *Metab. Eng. 38*, 29−37.
(52) Trinh, C. T., and Srienc, F. (2009) Metabolic engineering of Escherichia coli for efficient conversion of glycerol to ethanol. *Appl. Environ. Microbiol. 75*, 6696−6705.
(53) Neidhardt, F. C., Ingraham, J. L., and Schaechter, M. (1990) *Physiology of the Bacterial Cell: A Molecular Approach*, Sinauer Associates, Sunderland, MA.
(54) http://parts.igem.org/Promoters/Catalog/Anderson
(55) Agarwal, P. K., Uppada, V., and Noronha, S. B. (2013) Comparison of pyruvate decarboxylases from Saccharomyces cerevisiae and Komagataella pastoris (Pichia pastoris). *Appl. Microbiol. Biotechnol. 97*, 9439−9449.
(56) Conrad, T. M., Lewis, N. E., and Palsson, B. Ø. (2011) Microbial laboratory evolution in the era of genome-scale science. *Mol. Syst. Biol. 7*, 509.
(57) Dragosits, M., and Mattanovich, D. (2013) Adaptive laboratory evolution−principles and applications for biotechnology. *Microb. Cell Fact. 12*, 64.
(58) De Gelder, L., Ponciano, J. M., Joyce, P., and Top, E. M. (2007) Stability of a promiscuous plasmid in different hosts: no guarantee for a long-term relationship. *Microbiology 153*, 452−463.
(59) Bouma, J. E., and Lenski, R. E. (1988) Evolution of a bacteria/plasmid association. *Nature 335*, 351−352.
(60) Higgins, S. A., Ouonkap, S. V. Y., and Savage, D. F. (2017) Rapid and Programmable Protein Mutagenesis Using Plasmid Recombineering. *ACS Synth. Biol.*, DOI: 10.1021/acssynbio.7b00112.
(61) Trinh, C. T., Carlson, R., Wlaschin, A., and Srienc, F. (2006) Design, construction and performance of the most efficient biomass producing E. coli bacterium. *Metab. Eng. 8*, 628−638.
(62) Gibson, D., Young, L., Chuang, R., Venter, J., Hutchison, C., and Smith, H. (2009) Enzymatic assembly of DNA molecules up to several hundred kilobases. *Nat. Methods 6*, 343−345.
(63) Anderson, J. C., Dueber, J. E., Leguia, M., Wu, G. C., Goler, J. A., Arkin, A. P., and Keasling, J. D. (2010) BglBricks: A flexible standard for biological part assembly. *J. Biol. Eng. 4*, 1.

DOI: 10.1021/acssynbio.7b00269
ACS Synth. Biol. 2018, 7, 187−199